# Study on Suppression of Frequency Fluctuation in Microgrid by Renewable Energy and Integrated Coal Gasification Combined Cycle

Yoshitaka Aita[1], Shin'ya Obara[1]

[1]Kitami Institute of Technology in Japan

**Abstract**: *Currently, in Japan, many of the electricity supply depends on thermal power plants, and the impact of the emitted greenhouse gas on global warming is regarded as a problem. Therefore, renewable energy that does not emit greenhouse gases during operation attracts attention, and introduction of renewable energy such as photovoltaic power generation and wind power generation is proceeding in Japan. However, output of renewable energy largely fluctuates depending on weather conditions, and there is a possibility that problems may occur in the power quality of the grid by interconnecting a large amount of renewable energy to the grid. Therefore, in this research, integrated coal gasification combined cycle (IGCC) is used as a power supply to compensate for output fluctuation of renewable energy. However, the introduction of IGCC as a compensating power supply has limitation in maintaining power quality. Therefore, introducing a flywheel into the system and increasing the inertial force of the system, strengthening the maintaining power of the system frequency and increasing the introduction amount of renewable energy. Therefore, in this paper, investigated the influence of change for system inertia force on the power quality (frequency) of the system by numerical analysis to increase the introduction amount of renewable energy.*

**Keywords:** *IGCC, renewable energy, coal, flywheel, etc.*

## 1. Introduction

Since the output power of renewable energy depends on the weather conditions, the influence on grid power quality becomes a problem due to increases the introduction capacity of renewable energy. In particular, since the output power of renewable energy does not have power synchronization, the frequency system can decreases as increasing the amount of renewable energy. For this reason, in order to keep maintain the frequency fluctuation in this system, besides needed a limitation value of installing number when increasing the capacity of renewable energy, a good compensation power supply such as battery, flywheel, and others is also necessary for smoothing the output power. Thus, the proposed of this study is interconnecting the renewable energy and distributed IGCC in a wide area. IGCC that produces coal gasification fuel operates a combined cycle of gas turbine generator and steam turbine generator. Even though the power generation efficiency of conventional coal-fired power generation is getting around 48%, IGCC rises become 50%. While the fuel that containing the hydrogen as the main product, produced by separating carbon dioxide and recovering raw material through the water gas shift reaction that can be called coal gasification process [1]. As a result, the carbon dioxide emissions gas of IGCC per unit electricity generation are equal or less than that of natural gas thermal power generation. Therefore, IGCC claimed as a highly efficient and clean power generation method [2]. As refer to the analysis result of the previous study, a load following characteristics of electric power system that consisting of IGCC and renewable energy analysed by numerical analysis, becoming clear that the introduction renewable energy was limited for 10% of the maximum rated power of IGCC to keep maintain the power quality of the power system. Therefore, in order to increase the introduction capacity of renewable energy as the aim of this study, the flywheel will also introduce on the rotating shaft generator of IGCC. The introduction flywheel into the system not only can increases the inertia force of electric power system but also suppresses the supply/demand deviation and frequency fluctuation of the system. A dynamic characteristic model of the proposed system was created by using MATLAB / Simulink 2014a, while numerical analysis is performed by dividing the type of renewable energy, the introduction capacity, the introduction amount of the flywheel, etc. into various patterns. From the analysis result, it clarified the influence of the load follow-up performance of IGCC, the introducible capacity of renewable energy and the change of the inertia force of the system on frequency fluctuation of the system.

## 2. Coal gasification

The IGCC that used in this paper is oxygen-blown IGCC with the function of separating and recovering carbon dioxide, assuming an entrained bed gasification furnace. Coal of fuel is pulverized and supplied as a pulverized coal to the gasification furnace. At the same time supplying the Oxygen into the furnace, so that the pulverized coal instantaneously oxidizes to partial gas. The output gas from gasification furnace can be called raw material of synthesis gas and its composition as shown in Fig. 1(a). Then a raw material of synthesis gas is reformed by the water gas reaction as follows the Eq. (1). Because of the raw material of synthesis gas containing a lot of impurities and environmental pollutants, it is necessary to recover the $CO_2$ generation before supplying to the combustor. As a result, the low carbon content in the composition of syngas which supplies to the combustor as shown in Fig. 1(b) indicates that the amount of $CO_2$ emissions after combustion was reduce.

$$CO + H_2O \rightarrow CO_2 + H_2 \tag{1}$$

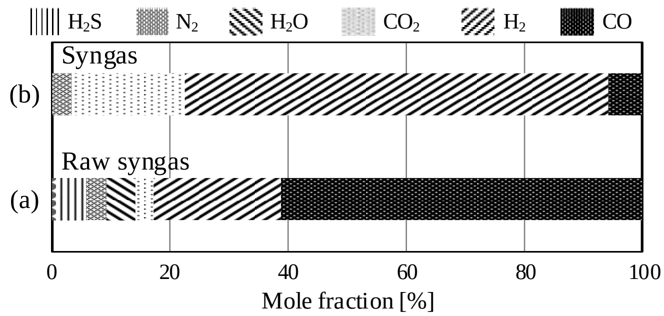


Fig. 1: Composition of syngas

## 3. Proposed System

### 3.1. System Configuration

The configuration of the proposed system is shown in Fig. 2. In this research, the photovoltaic power generation and wind power generation are assumed as renewable energy. In addition, the introduction ratio of photovoltaic power generation and wind power generation can be changed, and the inertial force of IGCC can be changed by installing a flywheel.

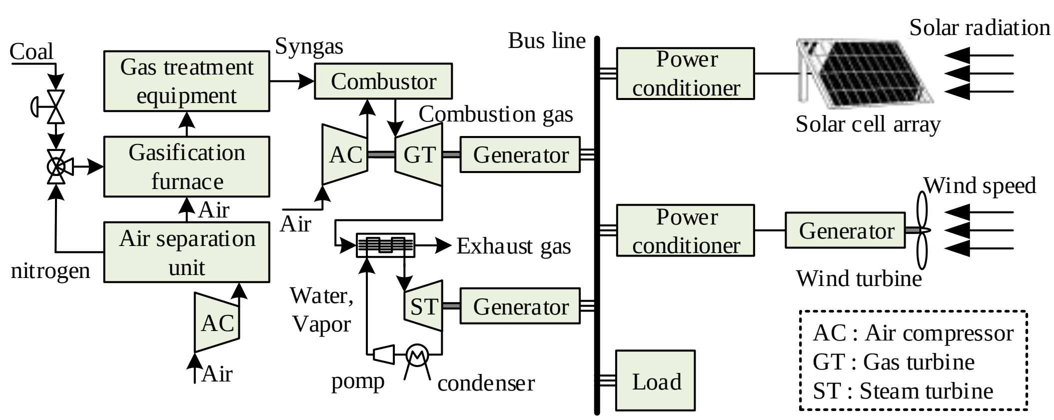


Fig. 2: System configuration

### 3.2. Frequency variation analysis model

In this analysis, a MATLAB/Simulink R2014a is used to create the model of IGCC, solar, and wind power generation. The Fig. 3, shows the frequency-variation analysis model of the proposed system.

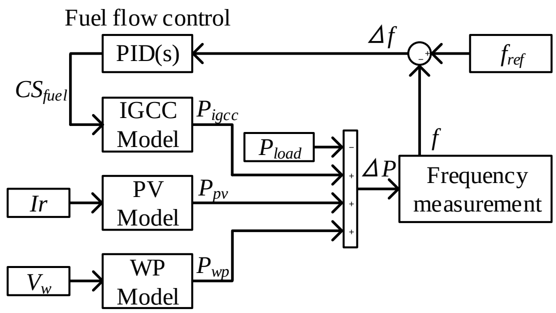


Fig. 3: Frequency variation analysis model

In the proposed system, the air compressor and the gas turbine are coaxial, and the mechanical output $P_{mgt}$ of gas turbine in IGCC as shown in Eq. (2), was calculated by subtracting the required work for air compressor from the energy of combustion gas that supplied from the combustor. The time delay of the air compressor also consider in Eq. (2). While to calculate the mechanical output $P_{mst}$ of steam turbine as shown in Eq. (3), the time delay of boiler will also consider. However, the output control was neglected in the steam turbine that used in this analysis. Then, the total output $P_{igcc}$ of IGCC as shown in Eq. (4). $P_{igcc}$ was obtained by multiplying the mechanical output $P_{mgt}$ of the gas turbine in Eq. (2) and the mechanical output $P_{mst}$ of the steam turbine in Eq. (3) by the efficiency of generator. In the Eq. (5) shows the output power $P_{pv}$ of photovoltaic generation model that obtained by multiplying the amount of solar radiation $I_{r,t}$, the wide-area $A_p$ of the photovoltaic power generation module, and the conversion efficiency $\eta_{pv}$. Whereas in the model of wind power generation, the output $P_{wp}$ for each wind generator calculated by using Eq. (6) then multiplied by the number of installation units to obtain the total output of wind power generation. Furthermore, the system frequency $f$ calculating in Eq. (7) and Eq. (8). The frequency deviation $\Delta f$ which shown in Eq. (8) of the system arises from difference power supply-demand $\Delta P$ of the electric power.

$$P_{mgt} = \frac{K_{gt}\{(T_f - T_e) - (T_d - T_i)\}W}{1 + T_{cd}s} \tag{2}$$

$$P_{mst} = \frac{K_{st}T_e W}{1 + T_b s} \tag{3}$$

$$P_{igcc,t} = P_{mgt,t}\eta_G + P_{mst,t}\eta_G \tag{4}$$

$$P_{pv} = A_p \cdot I_{r,t} \cdot \eta_{pv} \tag{5}$$

$$P_{wp} = C_p \cdot \frac{1}{2}\rho A_w V_{w,t}^3 \tag{6}$$

$$f = f_{ref} + \Delta f \tag{7}$$

$$\Delta f = \Delta\omega \cdot f_{ref} = \frac{1}{Ms}\frac{1}{\omega}\Delta P \cdot f_{ref} \tag{8}$$

# 4. Numerical analysis

## 4.1. Analysis content

The frequency-variation analysis of the proposed system consider through the following points below.

1) Table 1 shows the breakdown of introduction capacity of renewable energy in the proposed system. For the systems in Case 1, 2, and 3 of Table 1, investigates the introduction capacity of each renewable energy that can be introduced without installing the flywheel.
2) Introduce the introducible capacity of renewable energy obtained from the result of analysis 1) into the proposed system. Moreover, the inertial force of IGCC is changed by the introduction of the flywheel, and the frequency variation of the system is analysed. From the results, the suppression effect of frequency fluctuation accompanying the increase of inertia force will clarify.
3) The systems in Case 1, 2, and 3 of Table 1, will obtain the introducible capacity of renewable energy when changing the inertia force.

The inertial force of each system in analysis 1) is Pattern 1 in Table 2, and the inertial force of each system in the analysis 2), 3) is changed to 6 types from Pattern 2 to Pattern 7 in Table 2 and analysis is performed.

TABLE I: Breakdown of installed capacity of renewable energy

| Case | Photovoltaics | Wind power |
|---|---|---|
| Case 1 | 100 % | 0 % |
| Case 2 | 50 % | 50 % |
| Case 3 | 0 % | 100 % |

TABLE II: Analysis pattern

| Pattern | Inertial constant $M$ [s] | Moment of inertia $J$ [kg$\cdot$m$^2$] |
|---|---|---|
| Pattern 1 | 20 | $50.7\times10^3$ |
| Pattern 2 | 30 | $76.0\times10^3$ |
| Pattern 3 | 40 | $101.4\times10^3$ |
| Pattern 4 | 50 | $126.7\times10^3$ |
| Pattern 5 | 60 | $152.1\times10^3$ |
| Pattern 6 | 70 | $177.4\times10^3$ |
| Pattern 7 | 80 | $202.8\times10^3$ |

## 4.2. Analysis condition

The analysis of each system is used to supply 250 MW constant load which is assumed as a maximum of electric demand load. Consequently, the maximum output power of IGCC should be around 250 MW, refer also to the equipment which still being commercially operated in Japan [3]. Then the requirement frequency 50 Hz ±0.3 Hz is specified by Hokkaido Electric Power Co. Whereas, the rated output of gas turbine generator determined as rated output of steam turbine generator, that is around 167 MW, and 83 MW which based on the general output ratio of combined cycle [4]. The initial value for inertia constant, *M*, of the IGCC was set about 20s.

The shortage of power supply by renewable energy in the Case 1, 2, 3 for each system, compensated by the power supply of IGCC. In addition, the assuming output power of renewable energy that used in the proposed system is close to actual operation, the solar radiation and wind speed data input are estimated by weather data as shown in Fig. 4. When concentrating in one place of photovoltaic power generation, output change of about 70% occurs in 10 seconds. However, it is known that output fluctuation can be smoothed to 20% or less in 10 seconds by distributing photovoltaic power generation over a wide area [5]. Therefore, the amount of solar radiation amount data shown in Fig. 4(a) was prepared to satisfy the above conditions. Likewise, it has been reported that the output fluctuations are smoothed since the minute fluctuations of the wind power generators are dispersed in a wide area to cancel each other's small fluctuations [6]. Therefore, the wind speed data shown in Fig. 4 (b) was prepared to satisfy the above conditions. In this way, the meteorological data (Fig. 4) used for the analysis takes into account the accustomed effect, and analyses the frequency fluctuation in the Case 1, 2, 3 system using this weather data.

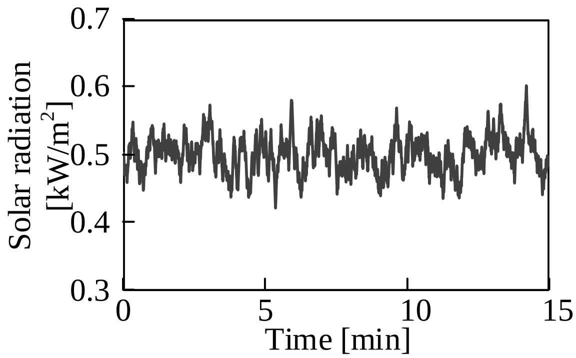

(a) Solar radiation

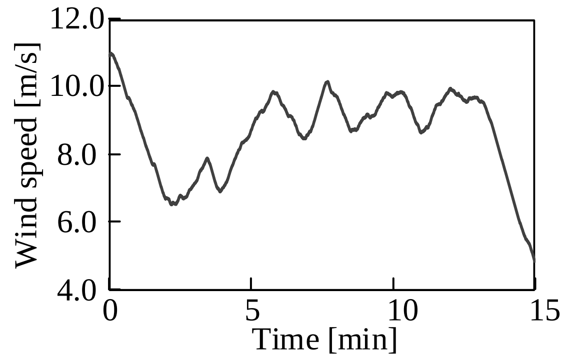

(b) Wind speed

Fig. 4: Input data

### 4.3. Analysis Result

Fig. 5(i) shows the analysis results of frequency fluctuation when photovoltaic power generation was introduced at 25.5 MW (corresponding to 10.2% of the rated output of IGCC) in the system of Case 1 in Table 1. Fig. 5(ii) shows the analysis results of the frequency fluctuation in Case 2 when the total capacity of renewable energy set around 5.80 MW (corresponding to 2.32% of the rated output of IGCC). Then, in the analysis result of Case 3 in Fig. 5(iii), shown when 3.10 MW capacity of wind power generation, (corresponding to 1.24% of the rated output of IGCC) introduced in the system. The frequency fluctuation result as shown in Fig. 5(i), Fig. 5(ii) and Fig. 5(iii) is within in the allowable range. Therefore, the installable capacity of photovoltaic power generation in the system of Case 1 is about 25.5 MW without introduction of flywheel. Further, the installable total capacity of photovoltaic power generation and Wind power generation in the system of Case 2 is about 5.80 MW without introduction of flywheel. Similarly, the installable capacity of Wind power generation in the system of Case 3 is about 3.10 MW without introduction of flywheel.

Further, in the Case 1 system, the introduction capacity of photovoltaic power generation is set to 25.5 MW with analysis results of frequency variation in the case of each inertial constant shown in Table 2 are shown in Fig. 6. While the system in Case 2, the introduction capacity of photovoltaic power generation and Wind power generation are sets to 5.80 MW with analysis results of frequency variation in the case of each inertial constant shown in Table 2 are shown in Fig. 7. At the same time in the Case 3, the introduction capacity of Wind power generation is set to 3.10 MW, and the analysis results of frequency fluctuation in the case of each inertial constant shown in Table 2 as shown in Fig. 8.

In the Case 1 system, frequency fluctuations are suppressed as the inertial force of the system increases as considered to the time of fluctuation by photovoltaic generation, in minute, that could be sufficiently suppressed as the inertial force increased. In the system of Case 2 and Case 3, the effect of suppressing frequency fluctuation due to the increasing the inertial force of the system was not much obtained. This is because wind power generation has a larger output fluctuation in a few minutes than photovoltaic power generation, and the flywheel greatly exceeds the corresponding variation amount. However, as with the case of Case 1, when the inertial force increases, a minute frequency fluctuation was suppressed to several tens of seconds.

Afterwards, in Fig. 9 summarizes the maximum frequency deviations of the analysis results as shown in Fig. 6, 7 and 8. In the case of Case 1, it can be confirmed that the maximum frequency deviation decreases with the increase of the inertial force of the system. However, as the inertial constant increased, the effect of suppressing frequency fluctuation will reduce automatically, and suppression of the frequency fluctuation due to the increase of the inertial force is considered to be limited. In the systems of Case 2 and Case 3, the smallest frequency deviation was obtained when the inertial constant is 40 [s]. Whereas in the Case 3 system, when the inertial constant is set around 50 [s] or more, the maximum frequency deviation increases automatically, resulting in deviating from the allowable range of the frequency fluctuation.

In Fig. 10 described the introducible ratio of renewable energy of each system as shown in Table 2 (based on the rated output of IGCC). In the Case 1 system, by increasing the inertia constant to become 2-4 times, the introduction rate of photovoltaic power generation increases by 1.9 times, 2.2 times, 2.8 times. Also, when the inertial constant set about 80 [s], the installable capacity of photovoltaic power generation becomes maximum, and 71.5 MW corresponding to 28.6% of IGCC rated power, 250 MW can be introduced. For system in Case 2, when the inertial constant set about 40 [s], the introduction capacity of photovoltaic power generation and wind power generation is maximized, photovoltaic power generation corresponding to 1.32% of IGCC rated output of 250 MW, 3.30 MW, rated IGCC Wind power generation 3.30 MW corresponding to 1.32% of output 250 MW can be introduced. Whereas for system in Case 3, when the inertial constant is 40 [s], the installable capacity of photovoltaic power generation becomes maximum, and 3.48 MW corresponding to 13.9% of IGCC rated output 250 MW can be introduced.

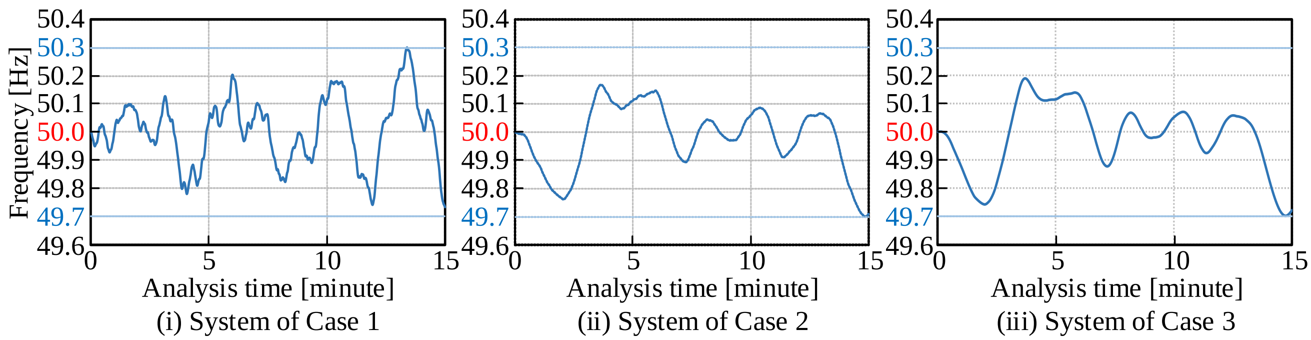


Fig. 5: Analysis result of frequency fluctuation (without flywheel)

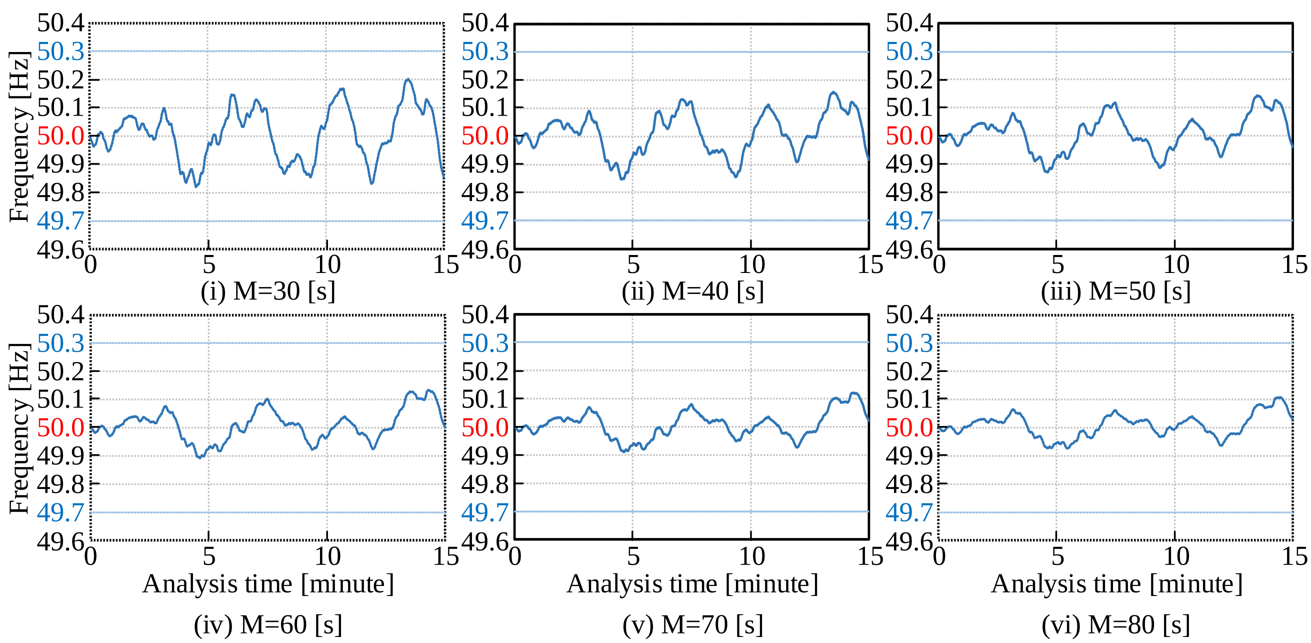


Fig. 6: Analysis result of frequency fluctuation due to change of inertial force (System of Case 1)

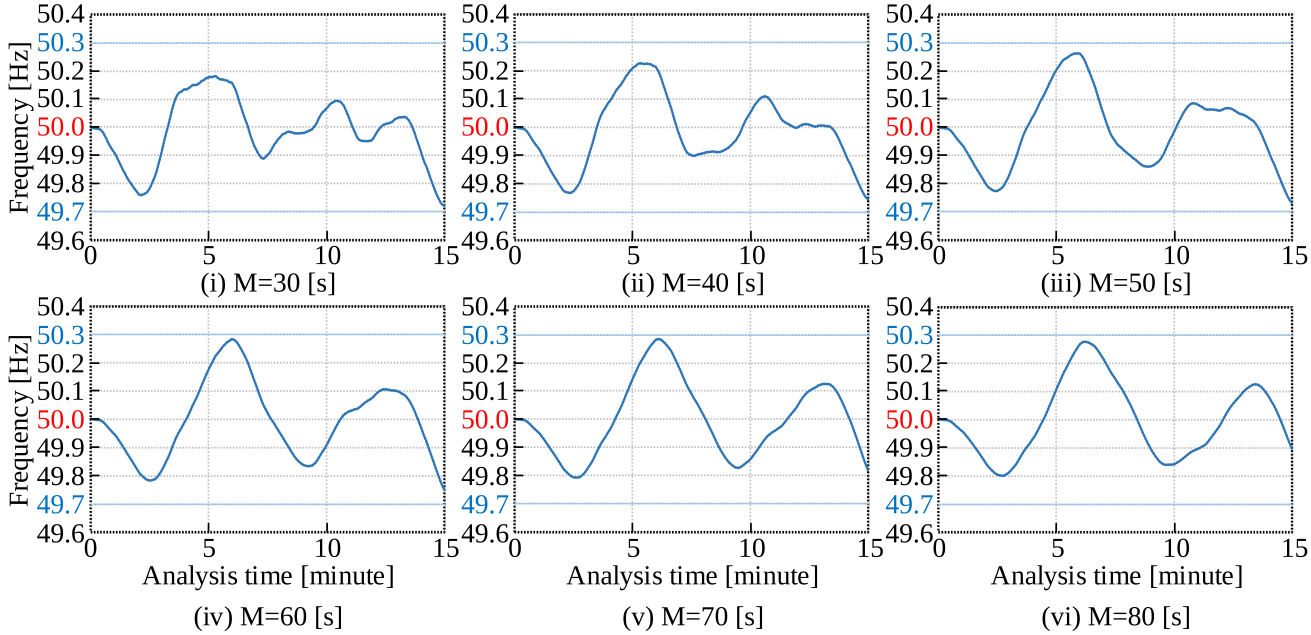


Fig. 7: Analysis result of frequency fluctuation due to change of inertial force (System of Case 2)

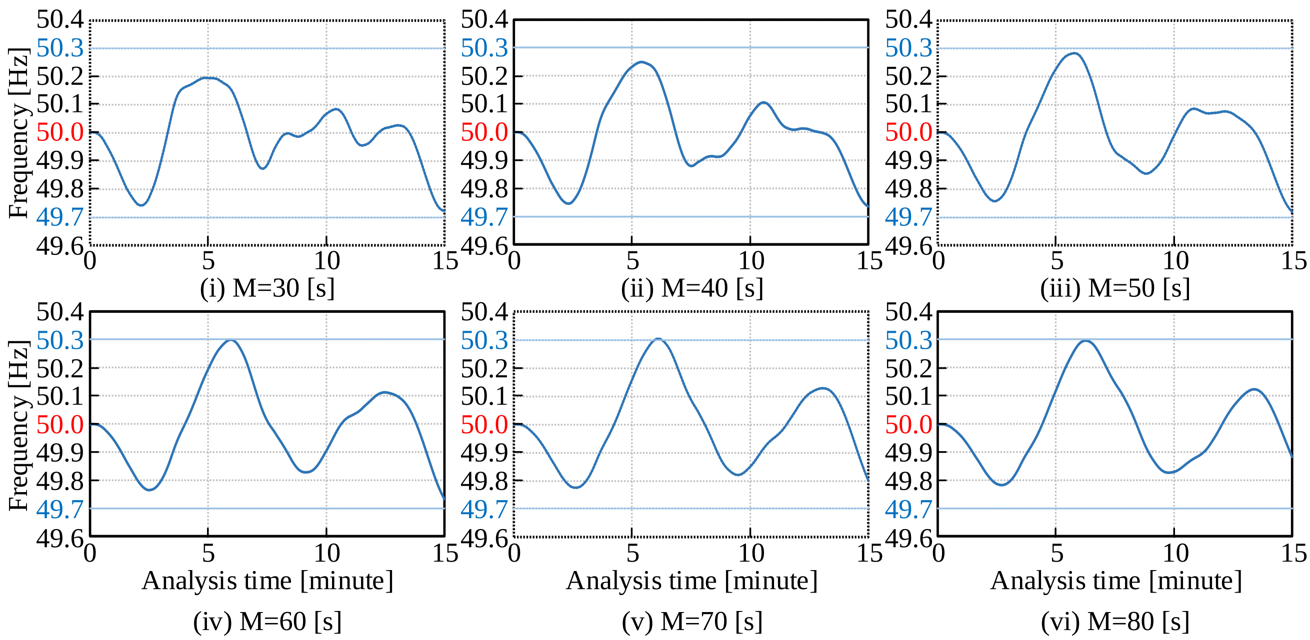


Fig. 8: Analysis result of frequency fluctuation due to change of inertial force (System of Case 3)

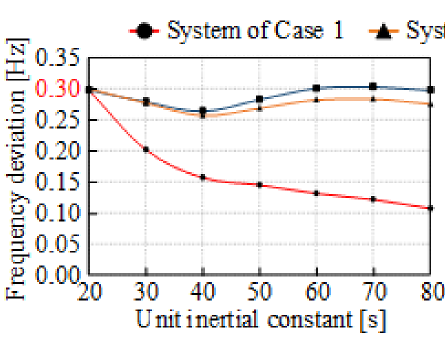


Fig. 9: Frequency deviation

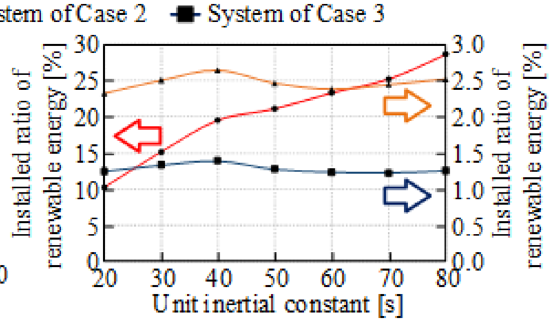


Fig. 10: Installed ratio of renewable energy

## 5. Conclusions

In this paper, a dynamic characteristic of IGCC was investigated with introduction of renewable energy by numerical analysis and clarified the capacity to introduce renewable energy from the analysis result of frequency variation. Furthermore, the frequency characteristics of the proposed system was also investigated, when the inertial force of IGCC was changed by introducing a flywheel. As a result, it became clear that frequency fluctuation was suppressed by increasing the inertial force of the system, and it is possible to increase the introduction capacity of renewable energy. However, there is a limitation to suppressing frequency fluctuation due to increasing the inertial force. Therefore, it is necessary to set appropriately the introduction capacity of flywheel according to the type and combination of renewable energy.

## 6. Graphic table

| | | | | | |
|---|---|---|---|---|---|
| $A_p$ | : | Area of photo voltaic module [$m^2$] | $T_b$ | : | Boiler delay time constant [s] |
| $A_w$ | : | Scavenging area of wind power [$m^2$] | $T_{cd}$ | : | Compressor delay time constant [s] |
| $C_p$ | : | Output coefficient of generator | $T_d$ | : | Compressor outlet temperature [K] |
| $f$ | : | System frequency [Hz] | $T_{do}$ | : | Compressor rated outlet temperature [K] |
| $f_{ref}$ | : | Rated system frequency [Hz] | $T_e$ | : | Gas turbine outlet temperature [K] |
| $I_{r,t}$ | : | Amount of solar radiation [$W/m^2$] | $T_f$ | : | Gas turbine inlet temperature [K] |
| $J$ | : | Moment of inertia [$kg{\cdot}m^2$] | $T_i$ | : | Outside air temperature [K] |
| $K_{st}$ | : | Steam turbine output coefficient | $t$ | : | Sampling time [hour] |
| $K_{gt}$ | : | Gas turbine output coefficient | $V_{w,t}$ | : | wind speed [m/s] |
| $M$ | : | Unit inertia constant [s] | $W$ | : | Air flow rate [pu] |
| $P_{igcc}$ | : | Total output of IGCC [MW] | $\eta_G$ | : | Generator efficiency |
| $P_{load}$ | : | Power demand [MW] | $\eta_{pv}$ | : | Conversion efficiency |
| $P_{mgt}$ | : | Mechanical output of gas turbine generator [MW] | $\rho$ | : | Air density [$kg/m^3$] |
| $P_{mst}$ | : | Mechanical output of steam turbine generator [MW] | $\omega$ | : | System frequency [pu] |
| $P_{pv}$ | : | Photo voltaic power output [MW] | $\Delta f$ | : | Frequency deviation [Hz] |
| $P_{wp}$ | : | Wind power generation output [MW] | $\Delta P$ | : | Demand difference [MW] |
| $S$ | : | Laplace operator | $\Delta\omega$ | : | System frequency deviation [pu] |

## 7. References


[1] Kristin, J., Rahul, A., Thijs, A.P., David, B., John, M., Petter, N., Rune, B.," High-purity H2 production with $CO_2$ capture based on coal gasification", Energy 88, 2015, pp. 9-17.

https://doi.org/10.1016/j.energy.2015.03.129

[2] Osamu, S., Akira, Y., Yoshinori, K.," The development of advanced energy technologies in Japan IGCC: A key technology for the 21st century", Energy Conversion and Management 43, 2002, pp. 1221-1233.

https://doi.org/10.1016/S0196-8904(02)00009-2

[3] Joban Joint Power Co., Ltd.," Current driving situation, issues and future developments of commercial facilities of integrated gasification combined cycle commercial facilities".

[4] Haruhito Taniguchi, Ohmsha, Ltd. EE Text, "Power system analysis - Modeling and simulation -".

[5] Shin'ya Obara, Yuta Utsugi, Yuzi Ito, Jorge Morel, Masaki Okada, "A Study on Planning for Interconnected Renewable Energy Facilities in Hokkaido, Japan", Applied Energy, Vol. 146, 2015.

[6] Agency for Natural Resources and Energy, Ministry of Economy, Trade and Industry," Accurate grasp of capacity capable of linkage of wind power generation from the viewpoint of frequency variation".